The Journal of Neuroscience, October 15, 2002, 22(20):8860–8868

Direct Effects of Calmodulin on NMDA Receptor Single-Channel Gating in Rat Hippocampal Granule Cells

Beth K. Rycroft and Alasdair J. Gibb

Department of Pharmacology, University College London, London WC1E 6BT, United Kingdom

NMDA receptors are glutamate-sensitive ion channel receptors that mediate excitatory synaptic transmission and are widely implicated in synaptic plasticity and integration of synaptic activity in the CNS. This is in part attributable to the high calcium permeability of the ion channel, which allows receptor activation to influence the intracellular calcium concentration and also the slow time course of NMDA receptor-mediated synaptic currents. NMDA receptor activity is also regulated by the intracellular calcium concentration through activation of various calcium-dependent proteins, including calmodulin, calcineurin, protein kinase C, and α-actinin-2. Here, we have shown that calmodulin reduces the duration of native NMDA receptor single-channel openings from 3.5 ± 0.6 msec to 1.71 ± 0.2 msec in agreement with previous studies on recombinant NMDA receptors (Ehlers et al., 1996). NMDA receptor single-channel amplitudes and shut times were not affected. However, calmodulin reduced the duration of groups of channel openings called superclusters, which determine the slow time course of synaptic currents, from 121 ± 25.4 msec to 60.4 ± 11.6 msec. In addition, total open time, number of channel openings, and charge transfer per supercluster were all reduced by calmodulin. A 68% decrease in charge transfer per supercluster suggests that calmodulin activation will significantly reduce calcium influx during synaptic transmission. These results suggest that calmodulin-dependent inhibition of NMDA receptors will reduce the amplitude and time course of excitatory synaptic currents and thus affect synaptic plasticity and integration of synaptic activity in the CNS.

Key words: NMDA receptors; calmodulin; hippocampus; dentate gyrus; granule cells; postnatal development; rat brain; patch-clamp

With progressive isolation and identification of many postsynaptic density elements, the biochemical basis for synaptic plasticity is becoming clearer (Kim and Huganir, 1999; Kennedy, 2000; Sheng and Pak, 2000). The NMDA receptor is a key component of the postsynaptic density and, because of its high calcium permeability (MacDermott et al., 1986; Mayer and Westbrook, 1987; Ascher and Nowak, 1988; Schneggenburger et al., 1993), has a significant role in synaptic plasticity (Bliss and Collingridge, 1993, 1995; Bear and Malenka, 1994).

Several calcium-dependent proteins associated with the postsynaptic density alter NMDA receptor activity, including calmodulin (CaM) (Ehlers et al., 1996; Hisatsune et al., 1997, Rafiki et al., 1997; Zhang et al., 1998; Krupp et al., 1999), calcineurin (Lieberman and Mody, 1994; Tong and Jahr, 1994; Tong et al., 1995), protein kinase C (PKC) (Chen and Huang, 1992; Wagner and Leonard, 1996; Xiong et al., 1998; Lu et al., 2000; Lan et al., 2001), and α-actinin-2 (Wyszynski et al., 1997; Zhang et al., 1998; Krupp et al., 1999). Therefore, it is generally acknowledged that calcium influx, in part through the NMDA channel, can regulate NMDA receptor activity via various pathways.

Calmodulin binds to two discrete regions of the NR1 subunit C terminus: a high-affinity site at the alternatively spliced C1 exon (estimated affinity, 4 nM) and a lower affinity site at the neighboring C0 region (estimated affinity, 87 nM) (Ehlers et al., 1996). Patch-clamp studies of recombinant NR1/NR2A receptors have shown that calmodulin reduces channel open time and open probability (P_{open}) (Ehlers et al., 1996). However, these results do not allow us to predict whether calmodulin will affect the time course of the synaptic current. For example, block of the channel by magnesium reduces channel open times and open probability but does not affect the synaptic current time course (Hestrin et al., 1990a).

Additional information concerning NMDA receptor function can be obtained from single-channel recordings by investigating the properties of groups of openings, referred to as "superclusters" (Gibb and Colquhoun, 1992; Wyllie et al., 1998). A supercluster constitutes a single receptor activation, the sequence of openings and closings between the first channel opening after agonist binding, and the last opening before complete dissociation of agonist (Gibb and Colquhoun, 1992). Single activations are of particular interest because there is good evidence that the NMDA receptor does not rebind glutamate during synaptic transmission (Hestrin et al., 1990b; Lester et al., 1990). The properties of single receptor activations, in combination with the first latencies to channel opening, will therefore determine the amplitude and time course of the synaptic current (Lester et al., 1990; Wyllie et al., 1998).

The effect of calmodulin on NMDA receptor-mediated synaptic currents has not been investigated directly, although Rosenmund et al. (1995) reported a calcium-dependent reduction in NMDA EPSC amplitude, and Umemiya et al. (2001) demonstrated a calcium-dependent shortening of the decay kinetics of NMDA miniature EPSCs. It is likely that calmodulin is involved in these effects (Zhang et al., 1998; Krupp et al., 1999).

In this study, we investigated the modulation of NMDA recep-

Received April 9, 2002; revised July 30, 2002; accepted July 31, 2002.

This work was supported by the Medical Research Council and the Wellcome Trust. We thank David Colquhoun for providing software.

Correspondence should be addressed to Dr. A. J. Gibb, Department of Pharmacology, University College London, Glower Street, London WC1E 6BT, UK. E-mail: a.gibb@ucl.ac.uk.

tor single-channel properties by calmodulin. The results demonstrate that calmodulin reduces NMDA channel mean open time, supercluster duration, total open time per supercluster, and the number of channel openings per supercluster, suggesting that calmodulin regulates the time course of the NMDA receptor-mediated synaptic current.

MATERIALS AND METHODS

Hippocampal slices (300 μm thick) from 12-d-old Sprague Dawley rats were made in an ice-cold (<4°C) oxygenated slicing solution of the following composition (in mM): 250 sucrose, 2.5 KCl, 1 $CaCl_2$, 4 $MgCl_2$, 1.25 NaH_2PO_4, 24 $NaHCO_3$, and 25 glucose, pH 7.4, using a vibroslicer (Vibroslice 752; Campden Instruments, Loughborough, UK). Slices were maintained for 1–8 hr at room temperature in an incubation chamber in Krebs solutions containing (in mM): 125 NaCl, 2.5 KCl, 1 $CaCl_2$, 4 $MgCl_2$, 1.25 NaH_2PO_4, 24 $NaHCO_3$, and 25 glucose, pH 7.4. Slices were viewed on the stage of an upright microscope (Zeiss Axioscope FS; Oberkochen, Germany) using Nomarski differential interference contrast optics (Edwards et al., 1989), and dentate gyrus granule cells were identified by their location, size, and morphology (Koh et al., 1995).

For single-channel recording, slices were bathed in Mg-free Krebs solution containing (in mM): 125 NaCl, 2.5 KCl, 1 $CaCl_2$, 1.25 NaH_2PO_4, 24 $NaHCO_3$, and 25 glucose, pH 7.4, continuously gassed with a mixture of O_2 (95%) and CO_2 (5%). Control outside-out patch recordings were made with patch pipettes filled with a low chloride (10 mM) pipette solution containing (in mM): 10 NaCl, 10 EGTA, 10 HEPES, and 140 sodium gluconate acid, adjusted to pH 7.3 with NaOH (Gibb and Colquhoun, 1991), with a buffered free calcium concentration (calibrated with a calcium electrode) of 12 nM. Total [Ca^{2+}], 5.32 mM, was calculated using the program "ALEX" by Michael Vivaudou (Biophysique Moleculaire et cellulaire, Centre National de la Recherche Scientifique, Grenoble, France), which is based on that described by Fabiato (1988).

Calmodulin has four calcium binding sites where occupancy of two or more binding sites is needed to give active calmodulin (James et al., 1995). The concentration of active calmodulin (calmodulin with two or more binding sites occupied) was calculated using the equilibrium constants for calcium binding given by Haiech et al. (1981) of K_1 = 67 nM, K_2 = 170 nM, K_3 = 600 nM, and K_4 = 900 nM. Active calmodulin (12 nM) was thus obtained at a total pipette concentration of 1.2 μM calmodulin. The affinity of calmodulin for a fusion peptide of the NR1 subunit C-terminal C1 region estimated by Ehlers et al. (1996) to be 4 nM suggests that 12 nM active calmodulin would result in 75% occupancy of the NR1 subunit high-affinity C1 region, whereas an estimated affinity of ~80 nM for the low-affinity C0 region would result in 13% occupancy by 12 nM active calmodulin.

Outside-out patch-clamp single-channel recordings were made with patch pipettes pulled from thick-walled aluminosilicate glass capillaries containing internal filament (SM150F-7.5; outer diameter 1.5 mm, inner diameter 0.80 mm; Clark Electromedical, Reading, UK) coated with Sylgard 184 (Dow Corning, Midland, MI) and fire polished on a microforge (Narishige MF-83; Tokyo, Japan) to a final resistance of 20–30 MΩ. Single-channel currents were recorded using a Axopatch 200A patch-clamp amplifier (Axon Instruments, Foster City, CA) and stored on digital audio tape (BioLogic DTR 1202). Before recording was attempted, the patch noise level was checked, and an rms noise level of <0.300 pA at a bandwidth of 5 kHz was considered acceptable. Patches showing spontaneous channel activity in the absence of agonists were discarded. Each outside-out patch was exposed to a constant low concentration of 10 μM glycine and 100 nM to 10 μM NMDA (Tocris Cookson, Bristol, UK) for 10–40 min at a membrane potential of −60 mV at room temperature (20–24°C).

Single-channel currents were replayed from tape, amplified and filtered at 2 kHz (eight pole Bessel), and digitized at 20 kHz using an analog-to-digital converter (CED 1401plus; Cambridge Electronics Design, Cambridge, UK). Each digitized record was analyzed using "SCAN", an interactive computer program (can be requested at http://www.ucl.ac.uk/Pharmacology/dcpr95.html) that fits the time course of each event based on the step response of the recording system (Colquhoun and Sigworth, 1995). Display and analysis of single-channel data distributions were done using "EKDIST" (Colquhoun and Sigworth, 1995). Before analysis, a fixed resolution for open times and closed times that gave a false event rate of $\leq 10^{-12}$ events/sec was imposed (Colquhoun and Sigworth, 1995). This was 100 μsec for open and closed times for the patches analyzed in this study. Before a patch was accepted for detailed analysis, the long-term stability of the data records was checked by making stability plots for amplitudes, open times, shut times, and P_{open} (Weiss and Magleby, 1989). Stability plots for amplitudes were made by plotting against event number, the amplitude of all openings longer than two filter rise times (332 μsec), which were therefore of a duration sufficient to reach ≥98.8% of their full amplitude. Each data point on the amplitude stability plot therefore represents a single-channel opening independent of its duration. Stability plots for open and shut times were made by calculating a moving average of 50 consecutive open or shut time intervals with an overlap of 25 events and plotting this average against the interval number at the center of the averaged values. Stability plots for open probability were made by calculating a P_{open} value for each set of 50 open and shut times. Once the stability of the record had been confirmed, amplitude distributions were made containing individual channel amplitudes longer than two filter rise times (332 μsec). Distributions of channel amplitudes were best fitted with the sum of two Gaussian components with the SD constrained to be the same for both components. Distributions of closed and open times were displayed using a logarithmic transformation of the *x*-axis (McManus et al., 1987; Sigworth and Sine, 1987) and a square root transformation of the *y*-axis (Sigworth and Sine, 1987). Distributions were fitted using the maximum likelihood method with probability density functions that were a mixture of three exponential components for open times and six exponential components for closed times (Colquhoun and Sigworth, 1995).

Superclusters of openings were defined as groups of openings separated by shut times of duration less than a critical shut time (Colquhoun and Sakmann, 1985), calculated from the fitted parameters of the distribution of shut times such that gaps underlying the sixth exponential component of the shut-time distribution were classified as gaps between superclusters (Gibb and Colquhoun, 1992; Wyllie et al., 1998). t_{crit} values were calculated so that the percentage of long shut times that were misclassified as "within clusters" was equal to the percentage of short shut times that were misclassified as "between clusters" (Colquhoun and Sigworth, 1995). Distributions of supercluster duration and total open time per supercluster were displayed with a square root scale on the *y*-axis and logarithmic scale on the *x*-axis and fitted with a mixture of exponential components. Distributions of the number of channel openings per supercluster were displayed with a square root scale on the *y*-axis and logarithmic scale on the *x*-axis (Anson et al., 2000) and fitted with a mixture of geometric components as appropriate. Supercluster P_{open} (the fraction of time during the supercluster that the channel dwells in any open state) was calculated for each experiment by dividing the mean total open time per supercluster by the mean supercluster duration. Mean charge transfer per supercluster was calculated by multiplying the weighted mean current amplitude by the mean total open time per supercluster.

Superclusters of openings (identified using the same t_{crit} value that was used to make distributions of superclusters) were aligned at the start of the first opening of each supercluster (Wyllie et al., 1998). Sections of the data record of a fixed length and containing only one supercluster were visually checked and stored for subsequent averaging. If the (fixed length) sample being averaged contained any other openings after the end of the supercluster, the openings were replaced by sections of empty baseline excised from nearby parts of the data record. Those containing simultaneous openings (double openings) were discarded.

Data are expressed as mean ± SE. For statistical comparisons, a randomization test was used that does not involve making any assumptions about the shape of the distribution of observations (can be requested at http://www.ucl.ac.uk/Pharmacology/dcpr95.html). Statistical significance was set at $p < 0.05$, unless otherwise indicated.

RESULTS

Single NMDA channel recordings

NMDA (100 nM to 10 μM) and a saturating concentration of glycine (10 μM) were applied to outside-out patches taken from hippocampal dentate gyrus granule cells to allow identification of individual NMDA receptor activations. In these experiments, calmodulin was present in excess (1.2 μM) in the pipette solution, and the calcium concentration (12 nM) was buffered to produce 12 nM active calmodulin (for more detail, see Materials and Methods). This concentration of active calmodulin was chosen to investigate the actions of calmodulin when predominantly bound

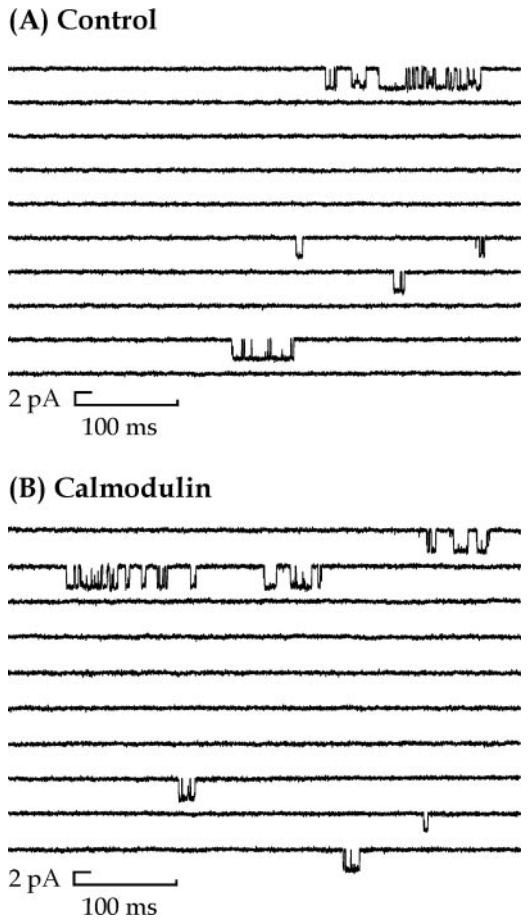

Figure 1. Patterns of channel activity mediated by NMDA receptors in control (*A*) and 12 nM calmodulin-treated (*B*) outside-out patches. Downward deflections in the baseline indicate single-channel openings in the presence of 100 nM NMDA and 10 μM glycine for *traces* in *A* and *B*. Recordings are from outside-out patches taken from dentate gyrus hippocampal granule cells. *Traces* in *A* and *B* show a 5 sec continuous recording at a holding potential of −60 mV. Currents were low-pass filtered at 2 kHz (−3 dB, 8 pole Bessel filter).

to the high-affinity C1 site on the NR1 subunit of the NMDA receptor (Ehlers et al., 1996).

Single-channel amplitude measurements at −60 mV gave a main chord conductance of 54.7 ± 1.1 pS and subconductance of 41 ± 0.8 pS for control patches (n = 13) and 57.2 ± 1.7 pS and 43.9 ± 1.5 pS for calmodulin-treated patches (n = 15), indicating that single-channel conductance was not significantly altered by the presence of calmodulin. These data are similar to those from previous experiments on granule cell NMDA receptors (Strecker et al., 1994).

To collect enough data to analyze groups of channel openings constituting a supercluster, recordings were maintained for ≤60 min depending on the level of channel activity. Figure 1 illustrates continuous recordings, each 5 sec in duration, from a control and 12 nM calmodulin-treated patch, respectively, recorded at −60 mV. The presence of 12 nM calmodulin applied to the intracellular surface of outside-out patches did not alter the long-term stability of NMDA channel amplitude or kinetic behavior, such as mean shut time, mean open time, and open probability, as illustrated in Figure 2.

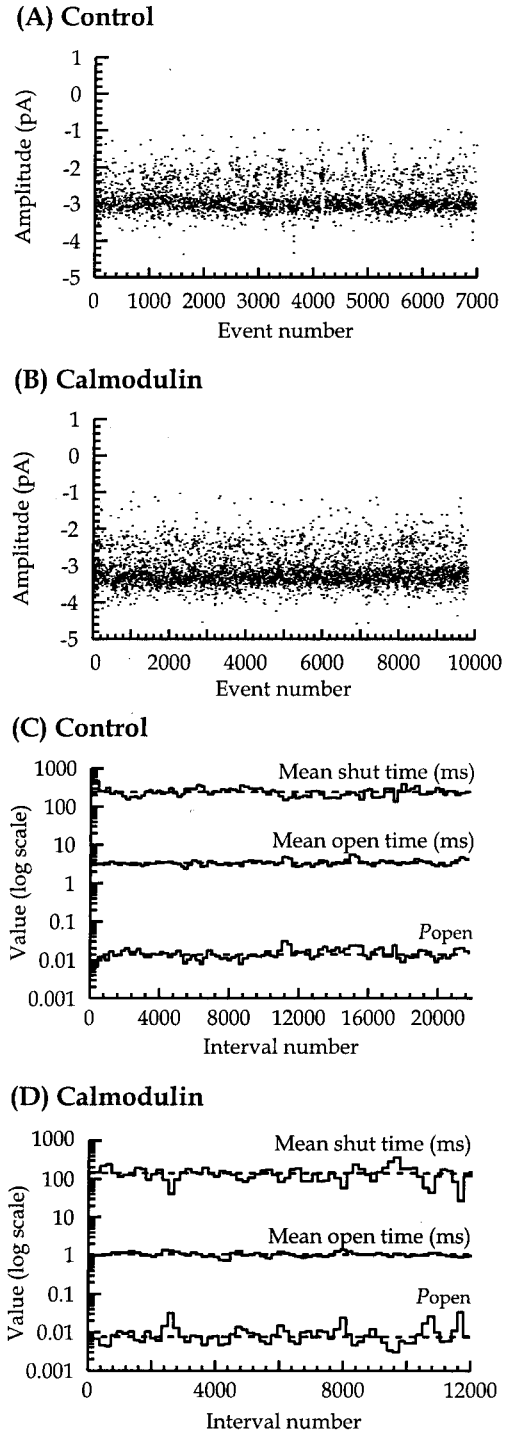

Figure 2. Stability plot analysis of single-channel amplitudes, shut times, open times, and P_{open} for control (*A*, *C*) and 12 nM calmodulin-treated patches (*B*, *D*). Amplitude stability plots contain 3449 (*A*) and 4998 (*B*) plotted amplitudes, for amplitudes longer than two filter rise times, observed during recordings of 840 sec (*A*) and 3648 sec (*B*) duration. Kinetic stability plots (*C*, *D*) show a running average of shut times (*top*), open times (*middle*), and P_{open} (*bottom*). Bins show a running average of 100 or 150 consecutive open or shut time intervals with an overlap of 50 or 75 events plotted against the interval number at the center of the averaged values. *Horizontal dashed lines* represent the average values for the whole recording. In these examples, the overall mean shut time, mean open time, and P_{open} were 240 msec, 3.39 msec, and 0.014 for control and 141 msec, 1.07 msec, and 0.008 for 12 nM calmodulin, respectively.

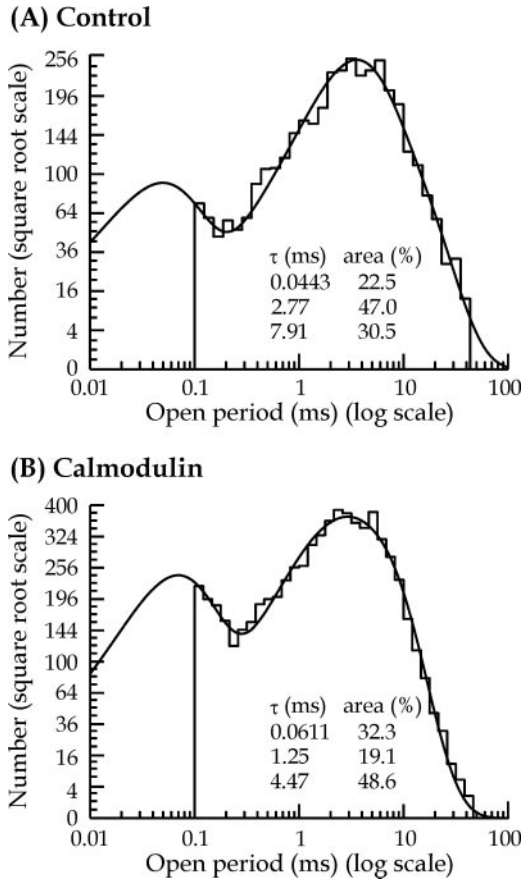

Figure 3. Comparison of distributions of open periods in control (*A*) and 12 nM calmodulin-treated (*B*) patches. In these distributions, open periods ranging from 0.1 to 59.9 msec were fitted with a mixture of three exponential components (time constants and associated areas are shown in the *inset*). The predicted mean open times (and observed and predicted number of observations) were 3.72 msec (3675 and 4719) for control and 2.43 msec (6641 and 9294) for calmodulin-treated patches.

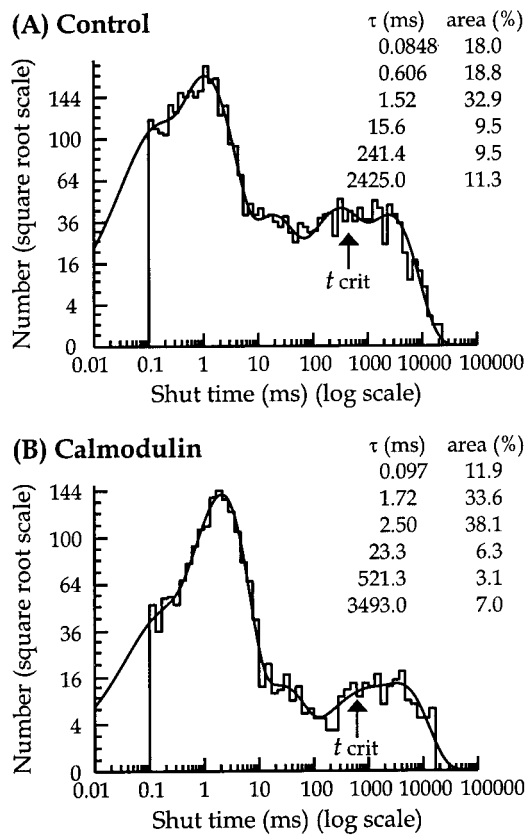

Figure 4. Distribution of shut times for control (*A*) and 12 nM calmodulin-treated (*B*) patches. In these distributions, shut time intervals ranging from 0.1 to 20,660 msec were best fitted with a mixture of six exponential components (time constants and associated areas are shown in the *inset*). The predicted mean shut times (and observed and predicted number of observations) were 299 msec (3744 and 4540) for control and 264 msec (1840 and 2069) for calmodulin-treated patches. Bisection of the fifth and sixth exponential components gave a t_{crit} value, indicated by an *arrow*, used in identifying superclusters of 407 msec for control and 562 msec for the calmodulin-treated patch in this instance.

Calmodulin reduces single NMDA receptor channel mean open time

Distributions of the duration of all channel openings during a single recording were best fitted with a mixture of three exponential components (Fig. 3). The mean time constants for each component (and relative area) were 96 ± 11 μsec (20 ± 3%), 2.12 ± 0.4 msec (33 ± 5%), and 5.84 ± 0.8 msec (47 ± 6%) for control patch data (n = 13) and 135 ± 32 μsec (29 ± 2%), 1.01 ± 0.1 msec (31 ± 6%), and 3.2 ± 0.3 msec (40 ± 5%) for calmodulin-treated patches (n = 15). Figure 2 illustrates that the presence of calmodulin appears to shift the NMDA single-channel open-time distribution to the left when compared with the control patch open-time distribution. This reflects a significant decrease in the NMDA receptor mean open time in the presence of calmodulin (1.71 ± 0.2 msec) when compared with control (3.5 ± 0.6 msec). Depending on whether there are other kinetic effects of calmodulin, these results imply that the action of calmodulin will be to reduce macroscopic NMDA receptor-mediated postsynaptic currents.

Calmodulin does not affect single NMDA receptor channel mean shut time

To determine whether calmodulin produces kinetic effects on NMDA channel gating, in addition to affecting channel open times, it is necessary to examine the distribution of channel shut times. Shut-time distributions were best fitted with a mixture of six exponential components for both control and calmodulin-treated patches (Fig. 4). The mean time constants (and relative area) were 65 ± 4 μsec (22 ± 3%), 0.53 ± 0.04 msec (16 ± 2%), 1.79 ± 0.25 msec (22 ± 4%), 21.5 ± 3.42 msec (13 ± 2%), 358 ± 105 msec (10 ± 2%), and 1499 ± 365 msec (17 ± 4%) for control (n = 13) and 69 ± 7 μsec (15 ± 2%), 0.52 ± 0.06 msec (15 ± 2%), 2.01 ± 0.35 msec (23 ± 4%), 18.7 ± 2.12 msec (13 ± 1%), 254 ± 45 msec (14 ± 3%), and 1241 ± 272 msec (20 ± 2%) for calmodulin-treated patches (n = 15). The values for each time constant and its relative area were consistent between the two experimental groups, which suggests that calmodulin does not affect NMDA receptor channel shut times. The mean shut time for control (234 ± 36 msec) was not significantly different from that of calmodulin-treated patches (245 ± 44 msec). Therefore, these results suggest that the main effect of low concentrations of calmodulin is to reduce the channel mean open time without affecting channel shut times.

Calmodulin changes the characteristics of superclusters of single-channel openings

To determine whether calmodulin affects the properties of groups of openings resulting from a single receptor activation, groups of

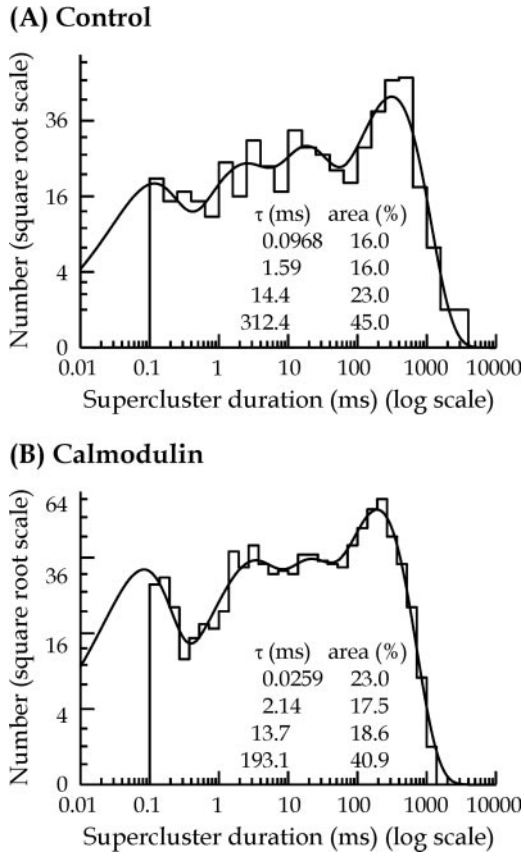

Figure 5. Comparison of supercluster length distributions for control (*A*) and 12 nM calmodulin-treated (*B*) patches. In these distributions, superclusters ranging from 0.1 to 2640 msec in duration were fitted with a mixture of four exponential components (time constants and associated areas are shown in the *inset*). Predicted mean supercluster duration (and observed and predicted number of observations) was 144 msec (512 and 578) for control and 40 msec (1041 and 1241) for the calmodulin-treated patch.

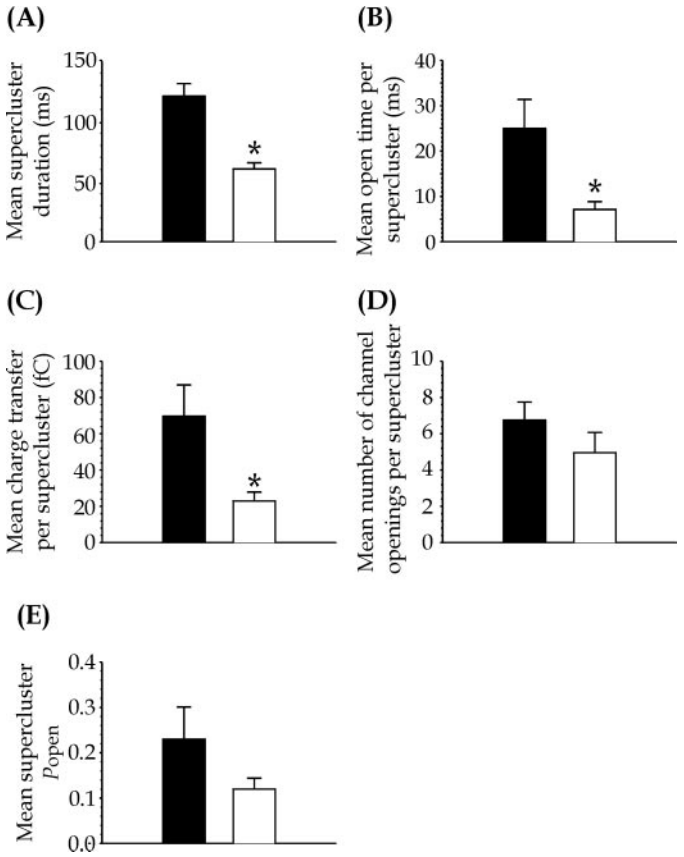

Figure 6. *A*, Comparison of mean supercluster length; *B*, mean open time per supercluster; *C*, mean charge transfer per supercluster; *D*, mean number of channel openings per supercluster; *E*, mean supercluster P_{open} for control and 12 nM calmodulin-treated patches. Bar charts illustrate averaged data for control (*black bars*) and calmodulin (*white bars*)-treated patches. Significant differences are indicated as follows: $^{*}p < 0.05$.

channel openings, here referred to as superclusters, were identified using the information contained within channel shut-time distributions. Superclusters were defined as groups of channel openings that are separated by shut periods shorter than a critical time (t_{crit}), which is calculated from the bisection of the fifth and sixth shut time components of the individual patch shut-time distributions, as illustrated in Figure 4.

Six control patches were suitable for supercluster analysis and five calmodulin-treated patches, based on clear separation of the fifth and sixth exponential components of the shut-time distribution. The mean t_{crit} was 294.4 ± 43.8 msec for control and 238.4 ± 49.8 msec for calmodulin-treated patches.

Distributions of supercluster durations were best fitted with a mixture of four exponential components (Fig. 5). The mean time constants for each component (and relative area) were 0.13 ± 0.03 msec (18 ± 2%), 2.52 ± 0.91 msec (17 ± 2%), 20.8 ± 8.3 msec (20 ± 5%), and 254.7 ± 34.3 msec (45 ± 6%) for control patch data ($n = 6$) and 0.11 ± 0.02 msec (27 ± 4%), 1.49 ± 0.46 msec (19 ± 3%), 15.7 ± 7.3 msec (19 ± 4%), and 162.3 ± 25.1 msec (35 ± 3%) for calmodulin-treated patches ($n = 5$). Calmodulin significantly reduced the mean supercluster duration from 120.9 ± 25.4 msec in control to 60.4 ± 11.6 msec for calmodulin-treated patches.

Figure 6, *A* and *B*, summarizes the effect of calmodulin on supercluster characteristics. In addition to supercluster duration, total open time per supercluster was significantly reduced from 25 ± 6.4 msec ($n = 6$) in control to 7.12 ± 1.7 msec ($n = 5$) in the presence of calmodulin. Consequently, calmodulin significantly reduced mean charge transfer per supercluster from 69.6 ± 17 fC in control ($n = 6$) to 22.9 ± 4.9 fC in calmodulin-treated patches ($n = 5$) (Fig. 6*C*), and there was also a reduction in the number of channel openings per supercluster from 6.75 ± 1 in control ($n = 6$) to 4.95 ± 1.1 in calmodulin-treated patches ($n = 5$) (Fig. 6*D*). The reduction in supercluster duration, total open time per supercluster, and number of openings per supercluster by calmodulin all contributed to a reduction in supercluster P_{open} [0.23 ± 0.07 for control ($n = 6$), and 0.12 ± 0.02 for calmodulin-treated patches ($n = 5$)], although this was not statistically significantly (Fig. 6*E*).

Alignment of superclusters

To simulate and illustrate the actions of calmodulin in relation to its likely effects on synaptic currents, superclusters were aligned at the start of the first channel opening and averaged to give an ensemble current. Figure 7, *A* and *B*, illustrates examples of superclusters, and their alignment, from a control and calmodulin-treated patch where the mean supercluster durations were 88.6 and 27.8 msec, respectively. The corresponding ensemble currents were normalized and superimposed on a faster timescale and amplified to show the difference between the slow

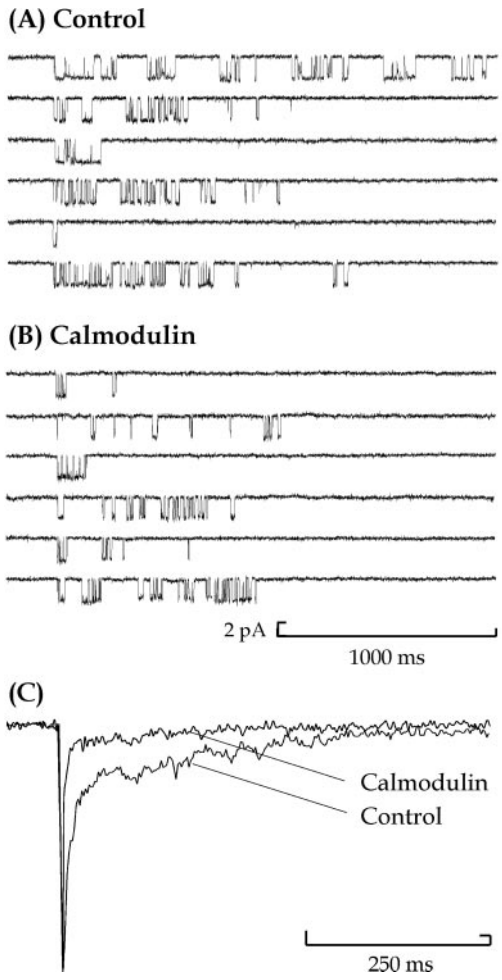

Figure 7. Alignment of superclusters of single NMDA channel activations. Sections of data records from control (*A*) and 12 nM calmodulin-treated (*B*) outside-out patches are presented. Each contains supercluster openings from patches exposed to 100 nM NMDA and 10 μM glycine. Each section of data record is 1100 msec long and contains a single supercluster of openings. These are aligned so that the start of the first opening of each supercluster occurs simultaneously. *C*, The corresponding ensemble currents are normalized and superimposed on a faster timescale (600 msec), and the normalized amplitudes are enlarged (238%) to show the difference between the slow component of the current decay for a control and a 12 nM calmodulin-treated patch, containing 643 and 1142 superclusters, respectively.

component of the current decay (Fig. 7*C*). These examples show that the average current from the calmodulin-treated patch has a faster decay time course than that of the control patch as expected from the properties of supercluster duration distributions.

DISCUSSION

We have shown that calmodulin regulates native NMDA receptor activity by reducing single-channel mean open time and the duration of superclusters of channel openings. A reduction in supercluster duration and total open time per supercluster indicates that calmodulin will inhibit NMDA receptor-mediated synaptic currents by shortening their decay time course and reducing their amplitude. This will influence the ability of a neuron to detect synchronous activity at two different synapses, as conferred by the NMDA receptor, a process important to the integration of synaptic inputs onto one neuron.

Inhibition of NMDA receptor single-channel activity by calmodulin

Although calmodulin significantly reduced NMDA receptor channel mean open time, the channel shut times remained unaffected. This suggests that an allosteric rather than a channel-blocking (Zhang et al., 1998) mechanism is involved in inhibition of single NMDA channel activity by calmodulin. For example, characteristic NMDA channel block, such as that observed with magnesium, is recognized by a distinct fingerprint alteration of the single-channel shut-time distribution (Ascher and Nowak, 1988; Antonov and Johnson, 1999). Because magnesium does not change the time course of NMDA receptor-mediated synaptic currents (Hestrin et al., 1990a), it is likely that a similar effect of calmodulin on the duration of channel activations will be observed at physiological magnesium concentrations (although the actions of calmodulin on channel open time would then be obscured by the much more rapid channel-blocking action of magnesium).

Because of the combined effect of calmodulin on channel open time and supercluster properties, mean charge transfer through the NMDA receptor channel during a single activation was reduced. Considering that calcium entry into the neuron contributes 16% of the NMDA receptor current (Schneggenburger et al., 1993), activation of intracellular second messenger systems that rely on this source of calcium will be altered by calmodulin.

To explain the mechanistic effect of calmodulin on supercluster properties, the following factors should be considered. The reduction by calmodulin of total open time per supercluster, and hence charge passed per supercluster, results from both a shortening of channel open time and a decrease in the number of openings per activation. Supercluster duration, however, depends on the open times, the number of openings, and the closed times within the activation. This is illustrated diagrammatically in Figure 8.

The duration of superclusters and the total open time per supercluster were reduced by 50 and 72%, respectively, in the presence of calmodulin. The difference between these two values reflects the presence of unaffected shut times included in the measurement of supercluster duration and the proportion of time the channel is open during the supercluster. Because the supercluster P_{open} is relatively low (0.1–0.2), the P_{open} does not change in proportion to changes in open time. However, overall, the reduction in the number of openings per supercluster combined with the reduction in mean open time is sufficient to significantly shorten the overall supercluster duration.

These results suggest that the effects of calmodulin can be described by assuming that calmodulin alters NMDA receptor gating, and we have tested this idea using simulations of channel activity (Colquhoun and Hawkes, 1995) based on the mechanism shown in Figure 8. This shows an extension of the mechanism proposed by Lester and Jahr (1992) to describe the time course of NMDA receptor-mediated synaptic currents and the response of NMDA receptors to rapid agonist application. By allowing calmodulin to bind equally well to any state in the Lester–Jahr model, the effects of calmodulin on single-channel activity observed in this study were simulated. This mechanism has some limitations in that it does not include the minimum of three open states and six shut states suggested by the single-channel data and so is used here only in a descriptive manner to illustrate the effects of calmodulin. In control recordings, the mean open time for patches selected for supercluster analysis was 3.67 msec,

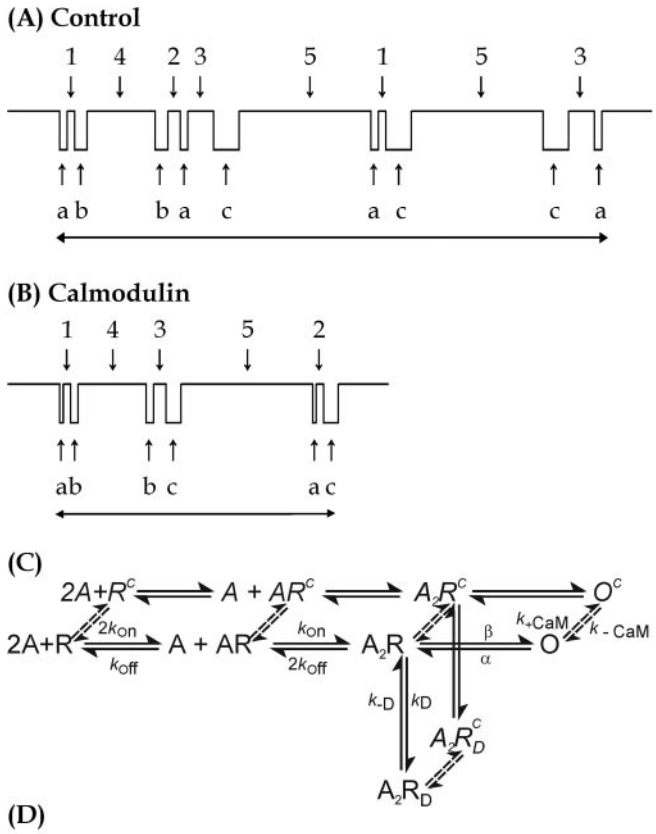

(D)

Rate constants				Control		CaM	
	Control	CaM		Model	Data	Model	Data
β	280 s^{-1}	150 s^{-1}	Number openings per supercluster	6.7	6.8	4.8	5.0
α	275 s^{-1}	2000 s^{-1}	Mean open time	3.6 ms	3.7 ms	1.7 ms	1.7 ms
k_D	1.8 s^{-1}	2.0 s^{-1}	Open time per supercluster	24.4 ms	25.0 ms	8.2 ms	7.1 ms
k_D	8.0 s^{-1}	3.0 s^{-1}	Supercluster length	120.0 ms	120.9 ms	62.5 ms	60.4 ms
			Supercluster *P* open	0.2	0.2	0.1	0.1

Figure 8. Illustration of the effects of calmodulin on supercluster duration. Shut time components *1*, *2*, *3*, *4*, and *5* (not drawn to scale) are unaffected by calmodulin, whereas channel open times *a*, *b*, and *c* are shortened, and the number of channel openings per supercluster is reduced, resulting in an overall reduction in supercluster duration and total open time per supercluster. A reduction in the number of openings per supercluster is associated with a reduced number of gaps per supercluster as illustrated schematically in *B*. *C*, An extension of the mechanism for NMDA channel gating proposed by Lester and Jahr (1992) is shown in which agonist (A) binds to receptor (R) that can be either free (R) or occupied by CaM (R^c). Doubly liganded receptor (A_2R) then isomerises to the open channel state (O) or to the desensitised state (A_2R_D). Calmodulin is assumed to be able to bind equally well to any state of the receptor ($k_{+CaM} = 10^{-6}$ M^{-1} sec^{-1} and $k_{-CaM} = 0.004$ sec^{-1}). Simulations of single-channel data, using the rate constants shown and with k_{on} and k_{off} fixed at 0.5×10^7 M^{-1} sec^{-1} and 25 sec^{-1}, resulted in supercluster properties that matched the data from control and calmodulin-treated patches as shown in *D*.

suggesting a channel closing rate, α, of 275 sec^{-1}. The channel opening rate, β, channel desensitization rate, k_D, and rate of recovery from desensitization, k_{-D}, were then set to give the number of openings per supercluster, supercluster duration, and supercluster P_{open} observed in control recordings. We assumed that the agonist, NMDA, has a microscopic association rate, k_{on} (0.5×10^7 M^{-1} sec^{-1}), and a dissociation rate, k_{off} (25 sec^{-1}), consistent with an equilibrium dissociation constant of 5 μM. These control rate constants were then fixed, and the calmodulin concentration was set to 12 nM with the association rate, k_{+CaM} (10^6 M^{-1} sec^{-1}), and dissociation rate, k_{-CaM} (0.4×10^{-2} sec^{-1}), consistent with the affinity of calmodulin for C1 estimated by Ehlers et al. (1996). By altering only the channel opening and closing rates and the rates into and out of the desensitized state of the calmodulin-bound receptor, it was then possible to mimic closely the supercluster properties observed in the presence of calmodulin. These results show that the effect of calmodulin can be reproduced by assuming that receptors with calmodulin bound have a 7.3-fold increased channel closing rate, 1.9-fold decreased channel opening rate, and 2.6-fold decreased rate of desensitization. The microscopic agonist association and dissociation rates need not be changed to simulate the effect of calmodulin, although these changes to the channel gating mean that the EC_{50} for NMDA is predicted to change from 2.9 to 5.6 μM in the presence of calmodulin. The results in this study do not test the possibility that glycine binding to the receptor could be affected by calmodulin or whether the action of calmodulin could be different at nonsaturating glycine concentrations. The glycine concentration used in this study (10 μM) is sufficient to saturate all but NR2A receptors. However, provided two glycine molecules must be bound for receptor activation to occur (Clements and Westbrook, 1991), then the results in this study suggest that the effect of calmodulin would be the same at other glycine concentrations. These considerations are also relevant to the fact that patch excision is known to prolong channel open times compared with the open times of cell-attached patches and removes glycine-sensitive desensitization (Sather et al., 1992) caused by the negative allosteric effect of agonist binding at the glutamate site on the glycine affinity at the glycine site (Benveniste et al., 1990). Although the rates of channel closing and desensitization are therefore likely to be different for receptors on an intact cell, the effect of calmodulin will remain.

Inhibition of NMDA-mediated synaptic currents by calmodulin

It is possible to predict that the time course of NMDA-mediated EPSCs will be close to the supercluster duration, because a synaptic current occurs in response to a brief pulse of glutamate in the synapse (Lester et al., 1990) and because the NMDA receptor does not rebind glutamate during synaptic transmission (Hestrin et al., 1990b; Lester et al., 1990). Because the first latencies (the time between agonist binding and first channel opening) are short relative to the supercluster duration (Jahr, 1992; Wyllie et al., 1998), the supercluster duration will be the main determinant of the synaptic current decay.

Wyllie et al. (1998) demonstrated that the time constants contained in the supercluster duration distribution are, in principal, similar to the time constants in the decay of a current produced by a very brief application of a high concentration of glutamate to outside-out patches. Because calmodulin reduced the time constants contained in the NMDA receptor supercluster duration

distributions, it follows that binding of calmodulin to the receptor will shorten the synaptic current.

To investigate this, macroscopic averaged currents were generated by the alignment of superclusters. In the presence of calmodulin, the decay time course was shortened, and the mean charge passed by the ensemble current was reduced. These results suggest that calmodulin will affect the role of the NMDA receptor in the computational aspects of neuronal function. Shortening of the NMDA EPSC by calmodulin will reduce the critical time period for temporal and spatial summation of synaptic inputs, their transmission to the axon hillock, and their interaction with back-propagating action potentials (Markram et al., 1997). This could alter the ability of two or more synchronized synaptic inputs to initiate action potentials. Inhibition of the NMDA synaptic current by calmodulin will reduce the interaction of presynaptic and postsynaptic activity and thus alter integration of synaptic activity. It has been shown that to strengthen the association of presynaptically evoked synaptic currents and postsynaptic action potentials in the dendritic tree, the two inputs must coincide within 100 msec in the neocortex (Markram et al., 1997). Considering that calmodulin shortens the decay of the EPSC, the time window for this form of integration would be reduced and fine-tuned by calmodulin.

The effect of calmodulin on NMDA receptor-mediated synaptic currents *in vivo* will depend on a number of factors. Phosphorylation of sites within the NR1 subunit C1 region by PKC (Leonard and Hell, 1997; Tingley et al., 1997) has been shown to alter calmodulin binding (Hisatsune et al., 1997). The ratio of phosphorylated/dephosphorylated NMDA receptors will also depend on the level of calcineurin activity. Because both PKC and calcineurin are calcium-dependent enzymes, their balance of activity will be determined by the intracellular calcium concentration (Mosior and Epand, 1994) and their respective activation and inactivation rates. In addition, the low-affinity calmodulin binding C0 region on the NR1 subunit of the NMDA receptor has been shown to contribute to calcium-dependent inactivation of whole-cell currents (Rafiki et al., 1997; Zhang et al., 1998; Krupp et al., 1999). Calmodulin bound to this second region on the NR1 subunit may therefore exert additional effects on NMDA channel kinetics and thus also alter the synaptic current. However, this latter point is complicated by competition for occupation of the NR1 subunit C0 region by the calcium-dependent, cytoskeletal protein α-actinin-2 (Zhang et al., 1998; Krupp et al., 1999).

The reduction in mean NMDA channel open time and number of openings per supercluster observed in the presence of a nanomolar concentration of calmodulin leads to a reduction in supercluster duration and total open time per supercluster. This causes a reduction in the mean charge passed by the NMDA receptor during a single activation. Overall, therefore, calmodulin-dependent NMDA receptor inactivation appears to serve two functions: shortening of the NMDA EPSC and attenuation of calcium influx through the NMDA receptor. The combination of these two processes will serve to modulate and fine-tune processes, such as synaptic plasticity, synaptic integration, and, therefore, neuronal computation.

REFERENCES

Anson LC, Schoepfer R, Colquhoun D, Wyllie DJ (2000) Single-channel analysis of an NMDA receptor possessing a mutation in the region of the glutamate binding site. J Physiol (Lond) 527:225–237.

Antonov SM, Johnson JW (1999) Permeant ion regulation of *N*-methyl-D-aspartate receptor channel block by Mg^{2+}. Proc Natl Acad Sci USA 96:14571–14576.

Ascher P, Nowak L (1988) The role of divalent cations in the *N*-methyl-D-aspartate responses of mouse central neurones in culture. J Physiol (Lond) 399:247–266.

Bear MF, Malenka RC (1994) Synaptic plasticity: LTP and LTD. Curr Opin Neurobiol 4:389–399.

Benveniste M, Clements J, Vyklicky Jr L, Mayer ML (1990) A kinetic analysis of the modulation of *N*-methyl-D-aspartic acid receptors by glycine in mouse cultured hippocampal neurones. J Physiol (Lond) 428:333–357.

Bliss TVP, Collingridge GL (1993) A synaptic model of memory: long-term potentiation in the hippocampus. Nature 361:31–39.

Bliss TVP, Collingridge GL (1995) Memories of NMDA receptors and LTP. Trends Neurosci 28:54–56.

Chen L, Huang LY (1992) Protein kinase C decreases magnesium block of the NMDA receptor channels as a mechanism of modulation. Nature 356:521–523.

Clements JD, Westbrook GL (1991) Activation kinetics reveal the number of glutamate and glycine binding sites on the *N*-methyl-D-aspartate receptor. Neuron 7:605–613.

Colquhoun D, Hawkes AG (1995) A Q-matrix cookbook: how to write only one program to calculate the single channel and macroscopic predictions for any kinetic mechanism. In: Single-channel recording, Ed 2 (Sakmann B, Neher E, eds), pp 589–636. New York: Plenum.

Colquhoun D, Sakmann B (1985) Fast events in single-channel currents activated by acetylcholine and its analogues at the frog muscle end-plate. J Physiol (Lond) 369:501–557.

Colquhoun D, Sigworth FJ (1995) Fitting and statistical analysis of single-channel records. In: Single-channel recording, Ed 2 (Sakmann B, Neher E, eds), pp 483–587. New York: Plenum.

Edwards FA, Konnerth A, Sakmann B, Takahashi T (1989) A thin slice preparation for patch clamp recordings from neurones of the mammalian central nervous system. Pflügers Arch 414:600–612.

Ehlers MD, Zhang S, Bernhardt JP, Huganir RL (1996) Inactivation of NMDA receptors by direct interaction of calmodulin with the NR1 subunit. Cell 84:745–755.

Fabiato A (1988) Computer programs for calculating total from specified free or free from specified total ionic concentrations in aqueous solutions containing multiple metals and ligands. Methods Enzymol 157:378–417.

Gibb AJ, Colquhoun D (1991) Glutamate activation of a single NMDA receptor-channel produces a cluster of channel openings. Proc R Soc Lond B Biol Sci 243:39–45.

Gibb AJ, Colquhoun D (1992) Activation of *N*-methyl-D-aspartate receptors by L-glutamate in cells dissociated from adult rat hippocampus. J Physiol (Lond) 456:143–179.

Haiech J, Klee CB, Demaille JG (1981) Effects of cations on affinity of calmodulin: ordered binding of calcium ions allows the specific activation of calmodulin-stimulated enzymes. Biochemistry 20:3890–3897.

Hestrin S, Nicoll RA, Perkel DJ, Sah P (1990a) Analysis of excitatory synaptic action in the rat hippocampus using whole-cell recording from thin slices. J Physiol (Lond) 422:515–533.

Hestrin S, Sah P, Nicoll RA (1990b) Mechanisms generating the time course of dual component excitatory synaptic currents recorded in hippocampal slices. Neuron 5:247–253.

Hisatsune C, Umemori H, Inoue T, Michikawa T, Kohda K, Mikoshiba K, Yamamoto T (1997) Phosphorylation-dependent regulation of *N*-methyl-D-aspartate receptors by calmodulin. J Biol Chem 272:20805–20810.

Jahr CE (1992) High probability opening of NMDA receptor channels by L-glutamate. Science 255:470–472.

James P, Vorherr T, Carafoli E (1995) Calmodulin-binding domains: just two faced or multi-faceted. Trends Biochem Sci 20:38–42.

Kennedy MB (2000) Signal-processing machines at the postsynaptic density. Science 290:750–754.

Kim JH, Huganir RL (1999) Organization and regulation of proteins at synapses. Curr Opin Cell Biol 11:248–254.

Koh DS, Geiger JR, Jonas P, Sakmann B (1995) Ca^{2+}-permeable AMPA and NMDA receptor channels in basket cells of rat hippocampal dentate gyrus. J Physiol (Lond) 485:383–402.

Krupp JJ, Vissel B, Thomas CG, Heinemann SF, Westbrook GL (1999) Interactions of calmodulin and α-actinin with the NR1 subunit modulate calcium-dependent inactivation of NMDA receptors. J Neurosci 19:1165–1178.

Lan J-Y, Skeberdis VA, Jover T, Grooms SY, Lin Y, Araneda RC, Zheng X, Bennett MVL, Zukin RS (2001) Protein kinase C modulates NMDA receptor trafficking and gating. Nat Neurosci 4:382–390.

Leonard AS, Hell JW (1997) Cyclic AMP-dependent protein kinase and protein kinase C phosphorylate *N*-methyl-D-aspartate receptors at different sites. J Biol Chem 272:12107–12115.

Lester RA, Jahr CE (1992) NMDA channel behavior depends on agonist affinity. J Neurosci 12:635–643.

Lester RA, Clements JD, Westbrook GL, Jahr CE (1990) Channel kinetics determine the time course of NMDA receptor-mediated synaptic currents. Nature 346:565–567.

Lieberman DN, Mody I (1994) Regulation of NMDA channel function by endogenous Ca^{2+}-dependent phosphatase. Nature 369:235–239.
Lu W-Y, Jackson MF, Bai D, Orser BA, MacDonald JF (2000) In CA1 pyramidal neurons of the hippocampus protein kinase C regulates calcium-dependent inactivation of NMDA receptors. J Neurosci 20:4452–4461.
MacDermott AB, Mayer ML, Westbrook GL, Smith SJ, Barker JL (1986) NMDA-receptor activation increases cytoplasmic calcium concentration in cultured spinal cord neurones. Nature 321:519–522.
Markram H, Lubke J, Frotscher M, Sakman B (1997) Regulation of synaptic efficacy by coincidence of postsynaptic APs and EPSPs. Science 275:213–215.
Mayer ML, Westbrook GL (1987) The action of *N*-methyl-D-aspartic acid on mouse spinal neurones in culture. J Physiol (Lond) 361:65–90.
McManus OB, Blatz AL, Magleby KL (1987) Sampling, log binning, fitting, and plotting durations of open and shut intervals from single channels and the effects of noise. Pflügers Arch 410:530–553.
Mosior M, Epand RM (1994) Characterisation of the calcium-binding site that regulates association of protein kinase C with phospholipid bilayers. J Biol Chem 19:13798–13805.
Rafiki A, Gozlan H, Ben-Ari Y, Khrestchatisky M, Medina I (1997) The calcium-dependent transient inactivation of recombinant NMDA receptor-channel does not involve the high affinity calmodulin binding site of the NR1 subunit. Neurosci Lett 223:137–139.
Rosenmund C, Feltz A, Westbrook GL (1995) Calcium-dependent inactivation of synaptic NMDA receptors in hippocampal neurons. J Neurophysiol 73:427–430.
Sather W, Dieudonne S, MacDonald JF, Ascher P (1992) Activation and desensitization of *N*-methyl-D-aspartate receptors in nucleated outside-out patches from mouse neurones. J Physiol (Lond) 450:643–672.
Schneggenburger R, Zhou Z, Konnerth A, Neher E (1993) Fractional contribution of calcium to the cation current through glutamate receptor channels. Neuron 11:133–143.
Sheng M, Pak DT (2000) Ligand-gated ion channel interactions with cytoskeletal and signalling proteins. Annu Rev Physiol 62:755–778.
Sigworth FJ, Sine SM (1987) Data transformations from improved display and fitting of single-channel dwell time histograms. Biophys J 52:1047–1054.
Strecker GJ, Jackson MB, Dudek FE (1994) Blockade of NMDA-activated channels by magnesium in the immature rat hippocampus. J Neurophysiol 72:1538–1548.
Tingley WG, Ehlers MD, Kameyama K, Doherty C, Ptak JB, Riley CT, Huganir RL (1997) Characterisation of protein kinase A and protein kinase C phosphorylation of the *N*-methyl-D-aspartate receptor NR1 subunit using phosphorylation site-specific antibodies. J Biol Chem 272:5157–5166.
Tong G, Jahr CE (1994) Regulation of glycine-insensitive desensitisation of the NMDA receptor in outside-out patches. J Neurophysiol 71:754–761.
Tong G, Shepherd D, Jahr CE (1995) Synaptic desensitization of NMDA receptors by calcineurin. Science 267:1510–1512.
Umemiya M, Chen N, Raymond LA, Murphy TH (2001) A calcium-dependent feedback mechanism participates in shaping single NMDA miniature EPSCs. J Neurosci 21:1–9.
Wagner DA, Leonard JP (1996) Effect of protein kinase C activation on the Mg^{2+}-sensitivity of cloned NMDA receptors. Neuropharmacology 35:29–36.
Weiss DS, Magleby KL (1989) Gating scheme for single GABA-activated Cl-channels determined from stability plots, dwell-time distributions, and adjacent-interval durations. J Neurosci 9:1314–1324.
Wyllie DJ, Behe P, Colquhoun D (1998) Single-channel activations and concentration jumps: comparison of recombinant NR1a/NR2A and NR1a/NR2D NMDA receptors. J Physiol (Lond) 510:1–18.
Wyszynski M, Lin J, Rao A, Nigh E, Beggs AH, Craig AM, Sheng M (1997) Competitive binding of the α-actinin-2 and calmodulin to the NMDA receptor. Nature 385:439–442.
Xiong ZG, Raouf R, Lu WY, Wang LY, Orser BA, Dudek EM, Browning MD, MacDonald JF (1998) Regulation of *N*-methyl-D-aspartate receptor function by constitutively active protein kinase C. Mol Pharmacol 54:1055–1063.
Zhang S, Ehlers MD, Bernhardt JP, Su C-T, Huganir RL (1998) Calmodulin mediates calcium-dependent inactivation of *N*-methyl-D-aspartate receptors. Neuron 21:443–453.